

## A bimodal catalytic membrane having a hydrogen-permselective silica layer on a bimodal catalytic support: Preparation and application to the steam reforming of methane

Toshinori Tsuru, Hiroaki Shintani, Tomohisa Yoshioka, Masashi Asaeda

Hiroshima University, Department of Chemical Engineering

1-4-1 Kagami-yama, Higashi-Hiroshima, 739-8527

E-mail: [tsuru@hiroshima-u.ac.jp](mailto:tsuru@hiroshima-u.ac.jp)

### Abstract

The steam reforming of methane for hydrogen production was experimentally investigated using catalytic membrane reactors, consisting of a microporous silica top layer, for the selective permeation of hydrogen, and an  $\alpha$ -alumina support layer, for catalytic reaction of the steam reforming of methane. An  $\alpha$ -alumina support layer with a bimodal structure, which was proposed for the enhanced dispersion of Ni catalysts, was prepared by impregnating  $\gamma$ -Al<sub>2</sub>O<sub>3</sub> inside  $\alpha$ -Al<sub>2</sub>O<sub>3</sub> microfiltration membranes (1  $\mu$ m in pore diameter), and then immersing the membranes in a nickel nitrate solution, resulting in a bimodal catalytic support. The bimodal catalytic support showed a large conversion of methane at a high space velocity compared with a conventional catalytic membrane with a monomodal structure. The enhanced activity of Ni-catalysts in bimodal catalytic supports was confirmed by hydrogen adsorption measurements. A bimodal catalytic membrane, i. e., a silica membrane coated on a bimodal catalytic support, showing an approximate selectivity of hydrogen over nitrogen of 100 with a hydrogen permeance of  $0.5\text{--}1 \times 10^{-5} \text{ m}^3 \text{ m}^{-2} \text{ s}^{-1} \text{ kPa}^{-1}$  was examined for the steam reforming of methane. The reaction was carried out at 500 °C, and the feed and permeate pressures were maintained at 100 and 20 kPa, respectively. Methane conversion could be increased up to approximately 0.7 beyond the equilibrium conversion of 0.44 by extracting hydrogen from the reaction stream to the permeate stream.

**Keywords:** Membrane reactor; Hydrogen; Bimodal catalytic membrane; Steam reforming of methane; Microporous silica membrane

## 1. Introduction

Hydrogen has attracted a great deal of attention for its possible applications to fuel cell systems, since it is a clean fuel and does not generate carbon dioxide on combustion. Hydrogen has been produced commercially by the steam reforming of hydrocarbons such as methane, and can be purified by distillation or pressure-swing adsorption. In the hydrogen production process, the steam reforming of methane (SRM), which is endothermic, and water gas shift reaction, which is endothermic, occur. Since both reactions are under thermodynamic equilibrium and the conversion of methane is limited, the reaction is conventionally operated at 800 °C, in order to complete the SRM reaction. Therefore, membrane reactors, in which both reaction and separation occur in one unit, have attracted a great deal of attention, since membrane reactors could be used to shift the equilibrium of the reaction by the selective extraction of hydrogen from the product stream, which would permit the process to be operated at a lower reaction temperature of 500 °C [1, 2].

Dense metal membranes such as Pd and Pd/Ag, which show 100% hydrogen permselectivity, have been used in hydrogen selective membranes [3, 4]. However, progress in the preparation of porous membranes such as porous silica membranes, which show a high selectivity of hydrogen over other gases such as CH<sub>4</sub>, has made it possible to utilize porous membranes for use in the reforming of methane [5-11]. In terms of membrane reactor configurations, packed-bed membrane reactors, which have packed-bed catalysts for the reaction and membranes for separation in one module, have been extensively investigated. On the other hand, a catalytic membrane, which has both catalytic activity and separation ability in one membrane, has attracted increasing attention due to the advantages associated with a more compact configuration than other types of membrane reactors. Catalytic membranes can be categorized into two types. The 1st type is a catalytic membrane in which the separation layer is inherently catalytically active like ZSM-5 zeolite membranes [1, 2, 12]. Another type is a catalytic membrane in which a separation layer and a catalytic layer are attached together

in one membrane. It should be noted that typical inorganic membranes have asymmetric structures; a thin separation layer is formed on a porous support, to reduce resistance of permeation. Therefore, catalytic membranes can be prepared by impregnating catalysts inside porous supports. The catalytic membrane has the advantage of compactness and ease of construction, compared with a packed-bed membranes reactor. Moreover, concentration polarization, which occurs on the membrane surface due to the selective extraction of hydrogen [13], can be decreased due to the close distance between the membrane and catalysts. In our previous papers [8, 10], a thin microporous silica layer which showed selective permeation to hydrogen, was formed on an  $\alpha$ -alumina support in which Ni-catalysts were impregnated, as schematically shown in Figure 1 (a), and was used in the steam reforming of methane. The thickness the catalytic  $\alpha$ -alumina support was approximately 1 mm, which had a closer configuration compared with a packed-bed membrane reactor and is suitable for reducing concentration polarization. However, the catalytic membrane reactor has one problem, that is, only a limited amount of catalyst can be impregnated in the membrane support. Therefore, the catalytic activity needs to be improved.

In the present paper, we propose a new type of catalytic membrane: a bimodal catalytic membrane, consisting of a separation layer and a bimodal catalytic layer, shown schematically in Figure 1 (b). Our previously reported catalytic membrane consisted of a separation layer and a catalytic layer in which the catalysts were impregnated inside macroporous supports. Figure 1 (b) shows a bimodal catalytic membrane consisting of a separation layer and a bimodal catalytic layer in which the catalytic support has a bimodal pore size distribution. A bimodal catalyst support, which contains both large and small pores, has a considerable advantage in solid catalysis reactions because the small pores contribute to the high dispersion of catalysts which enlarge the surface area of the support, and the large pores contribute to high molecular diffusion inside the catalyst [14-17]. A simple and new method for preparing bimodal catalytic supports was proposed by Fujimot et al [15, 16]. First,

colloidal sol solutions were initially introduced to macroporous supports, followed by drying and firing processes. Second, catalysts were impregnated by incipient-wetness using aqueous solutions of a metal salt. No attempts were made to apply this procedure to bimodal catalytic membranes.

In the present study, bimodal catalytic supports were prepared by forming mesoporous  $\gamma$ - $\text{Al}_2\text{O}_3$  inside cylindrical macroporous  $\alpha$ - $\text{Al}_2\text{O}_3$  microfiltration membranes, and followed by impregnation of a Ni-catalyst. An additional hydrogen permselective silica layer was deposited on the outer surface of the bimodal catalytic supports, resulting in bimodal catalytic membranes. The bimodal catalytic membranes were characterized by SEM, the Hg-intrusion method, nitrogen adsorption and hydrogen adsorption, and were then used in catalytic membrane reactions in the steam reforming of methane.

## **2. Experimental**

### **2.1 Preparation of bimodal catalytic supports and bimodal catalytic membranes**

Cylindrical  $\alpha$ - $\text{Al}_2\text{O}_3$  microfiltration membranes (outer diameter 10 mm, inner diameter 8 mm) with an average pore size of 1  $\mu\text{m}$  and an approximate porosity of 0.5, were used as a support. The  $\alpha$ - $\text{Al}_2\text{O}_3$  microfiltration membranes were soaked in boehmite sol solutions (Nissan Chemical Co., Japan), the concentration of which was adjusted in the range from 2 to 10 wt%. After removing the membranes from the solutions and wiping off excess amounts of boehmite solutions, they were dried at room temperature for several hours and then at 110 °C for 6 hours, followed by firing at 500 °C, resulting in bimodal supports. The bimodal supports were soaked in a 50 wt% of nickel nitrate solution, followed by drying and firing, resulting in bimodal catalytic supports, which will be abbreviated hereafter as Ni/Bimodal. For characterization of the catalytic supports,  $\alpha$ - $\text{Al}_2\text{O}_3$  cylindrical microfiltration membranes, which were cut into lengths of 3 cm, were used in the preparation of catalytic

supports. For the steam reforming of methane,  $\alpha$ -Al<sub>2</sub>O<sub>3</sub> cylindrical microfiltration membranes (9 cm in length) were used, both ends of which were connected to glass tubes; one end being sealed and the other end being used for the gas stream.

Bimodal catalytic membranes were prepared by coating Ni-doped silica colloidal sol solutions on the outer surface of bimodal catalytic supports. The procedure used to prepare silica colloidal sol solutions is as follows [18, 19]. Tetraethoxy silane (TEOS), mixed with nickel nitrate, and water, and ethanol with a nitric acid as a catalyst at molar ration of TEOS: Ni(NO<sub>3</sub>)<sub>2</sub>: H<sub>2</sub>O: HNO<sub>3</sub>: EtOH=0.9: 0.1: 4: 0.01: 10, was hydrolyzed for 12 hrs at room temperature. After adding additional nitric acid and water, the solutions were boiled for another 8 hrs to convert the polymeric sol to a colloidal sol solution. The outer surface of the bimodal catalytic supports were coated with  $\alpha$ -Al<sub>2</sub>O<sub>3</sub> particles (particle size 0.19  $\mu$ m; Sumitomo Chemical Industries Co., Japan) mixed with colloidal sol solutions to produce a sufficiently smooth surface for accepting a further coating of colloidal sol solutions, followed by a coating of colloidal sol solutions. Details of the preparation of the hydrogen separation layer can be found elsewhere [18, 19].

## 2. 2 Characterization

The bimodal catalytic supports were characterized by SEM (JEOL, Japan), nitrogen adsorption (BELLSORP 18, Bell, Japan), Hg-intrusion porosimetry (Shimadzu, AutoPore 9520, Japan), and hydrogen adsorption (Shimazu, Japan). For measurement of nitrogen adsorption, hydrogen adsorption and Hg-intrusion porosimetry, the catalytic supports were ground into powder, which was then used in the measurements. The amount of hydrogen adsorbed was measured by pulse-method; powdered samples of approximately 0.1 g were pre-treated in a stream of H<sub>2</sub> at 500 °C for 1 hr and the hydrogen was changed to argon (Ar), followed by decreasing the temperature down to room temperature in an Ar atmosphere. Hydrogen adsorption was measured at room temperature by injecting 1 ml of H<sub>2</sub>-N<sub>2</sub> and

monitoring the H<sub>2</sub> concentration using a TCD-gas chromatograph.

### 2.3 Steam reforming of methane

Figure 2 shows a schematic of the experimental apparatus used for the reactions in a membrane reactor. Before the reaction, the catalytic membranes were pretreated with hydrogen at 500 °C for 3 hrs. Mixtures of methane and water vapor, after mixing at a molar ratio of 3 (S/C=3), were fed inside a cylindrical catalytic membrane, since a separation layer was fabricated on the outer surface of the cylindrical catalytic membrane. The retentate and permeate stream were analyzed using two gas chromatographs (GC) with TCD detectors; one GC equipped with a Porapak T column, for the analysis of CO<sub>2</sub> and H<sub>2</sub>O, and the other with Molecular Sieve 5A, for H<sub>2</sub>, CH<sub>4</sub> and CO [10]. Two types of reaction configurations were examined: a pore-through type and a membrane reactor. The pore-through type reaction, in which all the feed gas was introduced to the permeate stream through the supports, was used to evaluate catalytic performance using bimodal catalytic supports. In the membrane reactor configuration, the feed stream was partially extracted to the permeate stream based on gaseous permeances and pressure differences between the feed and permeate streams, and flowed out to the retentate stream.

## 3. Results and Discussion

### 3.1 Characterization of bimodal catalytic supports

As shown in Figure 3 (a), the  $\alpha$ -Al<sub>2</sub>O<sub>3</sub> support consisted of several  $\mu$ m of  $\alpha$ -Al<sub>2</sub>O<sub>3</sub> particles. After impregnation of the Ni catalysts using aqueous solutions of nickel nitrate, Ni catalysts of several hundred nms in size were dispersed on  $\alpha$ -Al<sub>2</sub>O<sub>3</sub> particles, as shown in Figure 3 (b). Figure 3 (c) shows a bimodal catalytic support (Ni/Bimodal), i.e. a bimodal support impregnated with Ni catalysts.  $\gamma$ -Al<sub>2</sub>O<sub>3</sub> was found to be impregnated around the grain

boundaries of the  $\alpha$ -Al<sub>2</sub>O<sub>3</sub> particles and on the  $\alpha$ -Al<sub>2</sub>O<sub>3</sub> particles.

Figures 4 (a) and (b) show the pore size distributions for an  $\alpha$ -Al<sub>2</sub>O<sub>3</sub> support and a bimodal catalytic support (Ni/ Bimodal), respectively, determined by the Hg-intrusion method. Table 1 summarizes the pore volumes, surface areas and pore diameters together with the BET analysis. The  $\alpha$ -Al<sub>2</sub>O<sub>3</sub> support shows a sharp peak at 1 $\mu$ m, while the bimodal catalytic support shows a bimodal pore structure: a main peak at 0.92  $\mu$ m, corresponding to the original pore size of the  $\alpha$ -Al<sub>2</sub>O<sub>3</sub> support, and an additional peak at 7.5 nm. The BET analysis for a bimodal catalytic support and  $\gamma$ -Al<sub>2</sub>O<sub>3</sub> powder indicated average pore sizes of 4 nm. Therefore, the additional new peak observed for the Ni/ Bimodal was confirmed to be due to  $\gamma$ -Al<sub>2</sub>O<sub>3</sub> impregnated inside the  $\alpha$ -Al<sub>2</sub>O<sub>3</sub> support. A slight decrease in pore volume and macropore diameter is caused by the impregnation of Ni-catalysts. Although  $\gamma$ -Al<sub>2</sub>O<sub>3</sub> was impregnated only at 20 mg/g, the pore volume decreased from 0.20 to 0.18 ml/g, suggesting possible contribution of pore blocking by  $\gamma$ -Al<sub>2</sub>O<sub>3</sub>.

Nickel catalysts were assumed to be impregnated on the surface of  $\alpha$ -Al<sub>2</sub>O<sub>3</sub> and  $\gamma$ -Al<sub>2</sub>O<sub>3</sub> as well as inside  $\gamma$ -Al<sub>2</sub>O<sub>3</sub> mesopores. Since the amount of  $\gamma$ -Al<sub>2</sub>O<sub>3</sub> impregnated inside the macroporous  $\alpha$ -Al<sub>2</sub>O<sub>3</sub> support could be controlled by the concentration of the boehmite sol solutions and the impregnation times, bimodal catalytic supports having different amounts of impregnated  $\gamma$ -Al<sub>2</sub>O<sub>3</sub> were characterized. Figure 5 shows hydrogen adsorption, BET surface area, and the amounts of Ni impregnated as a function of the amounts of  $\gamma$ -Al<sub>2</sub>O<sub>3</sub>, which were controlled by the concentration of boehmite sol solutions in the range of 1-10 wt%. The amounts of impregnated Ni (as NiO) were approximately constant, irrespective of the amounts of impregnated  $\gamma$ -Al<sub>2</sub>O<sub>3</sub>, for the following reason. The pore volumes of the catalytic supports, which were prepared by impregnation of  $\gamma$ -Al<sub>2</sub>O<sub>3</sub>, were approximately constant, and amounts of Ni-impregnated were determined by the volume and concentration of nickel nitrate solutions which filled the pores of a bimodal support. On the other hand, the

BET surface areas increased approximately linearly with the amount of  $\gamma$ -Al<sub>2</sub>O<sub>3</sub> impregnated. This is because the impregnated  $\gamma$ -Al<sub>2</sub>O<sub>3</sub> had a large specific surface area and contributes to the increase in the observed surface area. The BET surface area of  $\alpha$ -Al<sub>2</sub>O<sub>3</sub> and Ni/ Bimodal (20 mg of impregnated  $\gamma$ -Al<sub>2</sub>O<sub>3</sub> to 1g  $\alpha$ -Al<sub>2</sub>O<sub>3</sub>) were 1.8 and 5.8 m<sup>2</sup>/g, respectively (Table 1). In terms of hydrogen adsorption, the amounts of adsorption increased drastically with the content of  $\gamma$ -Al<sub>2</sub>O<sub>3</sub>. The amount of H<sub>2</sub> adsorbed for Ni/  $\alpha$ -Al<sub>2</sub>O<sub>3</sub> and Ni/ Bimodal were 0.5 and 13 mmol/ g-support, respectively, which corresponds to the observed Ni-dispersion. Ni-dispersion, defined as the ratio of chemisorbed hydrogen atom to Ni atom, was found to be 0.4 and 5.5 %, respectively. After the impregnation of  $\gamma$ -Al<sub>2</sub>O<sub>3</sub>, the amount of H<sub>2</sub> adsorbed increased 15 times in comparison with that with  $\alpha$ -Al<sub>2</sub>O<sub>3</sub>, while the BET surface area increased only by 3 times. This strongly suggests that Ni-catalysts which were impregnated inside mesoporous  $\gamma$ -Al<sub>2</sub>O<sub>3</sub> were highly dispersed and would be expected to be active in catalytic reactions. Another point which should be addressed is gaseous permeances: the proposed bimodal catalytic supports need to also show high gaseous diffusivity. It should be noted that gaseous permeances through bimodal catalytic supports, the amount of impregnation of which was in the range of 0 to 20 mg/ g, showed negligible additional resistance to gaseous permeation, compared with gaseous permeance through  $\alpha$ -Al<sub>2</sub>O<sub>3</sub> the support. In conclusion, the structure of a bimodal catalytic support was confirmed to be as predicted in Figure 1 (b).

### 3.2 Bimodal catalytic membranes

Figure 6 shows a cross-sectional SEM photo of a bimodal catalytic membrane. As discussed above, a silica top layer for separation was coated on the outer surface of a cylindrical catalytic support. The permeances of hydrogen, helium, and nitrogen are shown in Figure 7. The permeance of hydrogen was  $1 \times 10^{-5} \text{ m}^3 \text{m}^{-2} \text{s}^{-1} \text{kPa}^{-1}$ , and the selectivity of hydrogen over nitrogen was 680. The permeance of helium and hydrogen showed activated



diffusion, where the permeance increased with temperature [20]. On the other hand, permeance of nitrogen was nearly constant, probably because nitrogen is assumed to permeate through relative large pores such as pinholes, which allowed the permeation of relatively large molecules such as nitrogen. After the hydrothermal treatment of the catalytic membrane (3 hr, the partial pressure of water: 50 kPa) the permeances of helium and hydrogen decreased, while that of nitrogen remained essentially constant. This is speculated to be because the hydrothermal treatment densified the micropores, which allowed the permeation of small molecules such as helium and hydrogen, through the process of the generation of silanol groups on the silica network and recombination to siloxane groups. On the other hand, large pores such as interparticle pores were not affected by the hydrothermal treatment or were slightly enlarged by the densification.

### 3.3 Catalytic activity of bimodal catalytic supports

The catalytic activities of the bimodal supports were evaluated in a flow-through type reaction where all of the reactant gas was forced to flow from the inside to outside of the cylindrical catalytic support with a thickness of 1 mm. Figure 8 (a) shows data for the conversion of methane as a function of methane feed flow rate. Conversion by a catalytic support impregnated with 0.21 g of NiO showed a higher conversion than that impregnated with 0.11 g due to the larger loading of Ni catalysts. However, methane conversion decreased with an increase in methane feed flow rate, irrespective of the amounts of Ni-impregnated. On the other hand, bimodal catalytic supports, the amounts of impregnated  $\gamma\text{Al}_2\text{O}_3$  of which were 9 and 38 mg, showed methane conversions with approximately constant values close to the equilibrium values. The lines in the figure indicate conversions at 100 and 120 kPa because the upstream pressure increased from 100 kPa to 120 kPa with an increase in the methane feed flow rate, while the down stream pressure was kept at atmospheric pressure (100 kPa). Although the amounts of Ni-impregnated were approximately 0.1 g, the activities were quite

sufficient, indicating that a high dispersion of Ni-catalyst was achieved by the impregnation of Ni catalysts into  $\gamma$ -Al<sub>2</sub>O<sub>3</sub>. The bimodal catalytic supports were confirmed to show enhanced catalytic activity due to the highly dispersed Ni-catalysts which were impregnated in  $\gamma$ -Al<sub>2</sub>O<sub>3</sub> mesopores.

### 3.4 Application to membrane reaction of steam reforming of methane

Figure 9 shows the time course for catalytic membrane performance. During the initial 160 min, the permeate stream was kept at atmospheric pressure ( $p_f=100$  kPa). No extraction occurred, and therefore, methane conversion, defined as the ratio of the sum of CO and CO<sub>2</sub> flow rate to that of CH<sub>4</sub>, CO, and CO<sub>2</sub>, was approximately 0.44, approximately the same as the equilibrium conversion. After evacuating the pressure of the permeate stream down to 20 kPa ( $p_f=20$  kPa), methane conversion was increased to 0.66, due to the effect of the extraction of hydrogen. Catalytic membrane performance using microporous membranes which allow the permeation of hydrogen as well as other gases based on molecular sieving effects, were simulated using a catalytic-membrane-reaction model. The simulation model, which is based on plug flow and isothermal conditions, is useful to predict catalytic membrane performances in terms of operation conditions (feed flow rate, reaction rate, pressure) as well as membrane conditions (hydrogen permeance, hydrogen selectivity, membrane area) [10, 21]. The lines shown in the figures were simulated under the assumption of an infinite reaction rate, using the permeances of hydrogen and water vapor, measured after reaction. Although the simulation was carried out without any other fitting parameters, the lines show good agreement with the experimental data.

Figure 10 shows methane conversion as a function of methane feed flow rate. Without membrane permeation, in which the permeate stream was kept at atmospheric pressure, the conversion was approximately equal to the value under equilibrium, irrespective of feed methane feed flow rate, thanks to the enhanced catalytic performance of the bimodal

support. With membrane permeation where the permeate stream was evacuated to 20 kPa, the conversion increased; methane conversion increased up to approximately 0.7 beyond the equilibrium conversion of 0.44 by extracting hydrogen from the reaction stream to the permeate stream. The reason why conversion increased with a decrease in methane feed flow rate can be explained as follows. The effect of extraction was enhanced by decreasing the feed flow rate since the flow rate of extraction by membrane is limited by the surface area of the membrane. After catalytic membrane reactions, the hydrogen permeance and the selectivity of nitrogen were decreased by densification of silica separation layer under the hydrothermal condition and/ or by the effect of reaction such as coke formation, which would be subject to further study. Calculated curves, using the permeances of hydrogen and water vapor, measured after reaction, are again in good agreement with the experimental data.

#### 4. Conclusions

A catalytic membrane reactor with a bimodal structure is proposed for enhancing the dispersion of Ni catalysts and applied for use in a membrane reaction of methane stream reforming.

1. Bimodal catalytic supports were prepared by impregnating  $\gamma$ -Al<sub>2</sub>O<sub>3</sub> inside  $\alpha$ -alumina microfiltration membranes, followed by impregnating nickel nitrate solutions. Hydrogen adsorption experiments suggested that the Ni-catalysts were highly dispersed in mesopores of the bimodal supports.
2. The flow-through reaction of the bimodal support revealed that a large conversion of methane at high space velocity were achieved, compared with that for a conventional catalytic support.
3. Bimodal catalytic membranes were prepared by the application of a further coating of Ni-doped silica colloidal sols solution on the bimodal catalytic support. The bimodal catalytic membranes showed a hydrogen permeance of  $1 \times 10^{-5} \text{ m}^3 \text{ m}^{-2} \text{ s}^{-1} \text{ kPa}^{-1}$ , and the selectivity of hydrogen over nitrogen was 680.
4. Mixtures of methane and water vapor at a molar ratio of 3 were fed inside the catalytic membranes at 500 °C under a feed side pressure of 100 kPa and a permeate pressure of

20 kPa. Methane conversion increased up to approximately 0.7 beyond the equilibrium conversion of 0.44 as the result of extracting hydrogen from the reaction stream to permeate stream.

5. Membrane reactor performances were simulated under the assumption of infinite reaction rate, using permeances of hydrogen and water vapor, and the simulation was in good agreement with experimental data.

### **Acknowledgement**

This work was partly supported by the R&D Project for High Efficiency Hydrogen Production/Separation System using Ceramic Membranes funded by the New Energy and Industrial Technology Development Organization (NEDO), Japan.

## References

- [1] J. G. Sanches, and T. T. Tsotsis, *Catalytic Membranes and Membrane Reactors*, Wiley-VCH (2002).
- [2] H. P. Hsieh, *Inorganic Membranes for Separation and Reaction*, Elsevier Science B. V. (1996).
- [3] S. Uemiyama, N. Sato, H. Ando, T. Matsuda, and E. Kikuchi, *Appl. Catal.*, **67** (1991) 223.
- [4] J. H. Kim, B. S. Choi, and J. Yi, *J. Chem. Eng. Jpn.*, **32** (1999) 760.
- [5] T. T. Tsotsis, A. M. Champagnie, S. P. Vasileiadis, Z. D. Ziaka, and R. G. Minet, *Sep. Sci. Tech.*, **28** (1993) 397.
- [6] A. K. Prabhu, and T. Oyama, *J. Membr. Sci.*, **176** (2000) 233.
- [7] A. K. Prabhu, A. Liu, L. G. Lovell, and T. Oyama, *J. Membr. Sci.*, **177** (2000) 83.
- [8] T. Tsuru, T. Tsuge, S. Kubota, K. Yoshida, T. Yoshioka, and M. Asaeda, *Sep. Sci. Tech.*, **36** (2001) 3721.
- [9] K. Yoshida, Y. Hirano, H. Fujii, T. Tsuru, and M. Asaeda, *Kagaku Kougaku Ronbunshu*, **27** (2001) 657.
- [10] T. Tsuru, K. Yamaguchi, T. Yoshioka, and M. Asaeda, *AIChE J.*, **50** (2004) 2794.
- [11] S. Kurugot, T. Yamaguchi, and S. Nakao, *Catal. Lett.*, **86** (2003) 273.
- [12] Y. Takata, T. Tsuru, T. Yoshioka, M. Asaeda, *Micropor. Mesopor. Mat.*, **54** (2002) 257.
- [13] S. Hara, K. Sakaki, N. Itoh, *Ind. Eng. Chem. Res.*, **38** (1999) 4913.
- [14] T. Numaguchi, *Catalysis Surveys from Japan*, **5** (2001) 59.
- [15] N. Tsubaki, Y. Zhang, S. Sun, H. Mori, Y. Yoneyama, X. Li, K. Fujimoto, *Catalysis Communications*, **2** (2001) 311.
- [16] Y. Zhang, Y. Yoneyama, K. Fujimoto, N. Tsubaki, *J. Chem. Eng. Japan*, **36** (2003) 874.
- [17] R. Takahashi, S. Sato, T. Sodesawa, K. Arai, M. Yabuki, *J. Catal.*, **229** (2005) 24.
- [18] M. Asaeda, and S. Yamasaki, *Sep. Pur. Tech.*, **25** (2001) 151.
- [19] M. Kanezashi and M. Asaeda, *J. Membr. Sci.*, *in press*.
- [20] T. Yoshioka, E. Nakanishi, T. Tsuru, and M. Asaeda, *AIChE J.*, **47** (2001) 2052.
- [21] T. Tsuru, K. Yamaguchi, T. Yoshioka, and M. Asaeda, *Kagaku Kougaku Ronbunshu*, **30** (2004) 346-352.

Table 1 Characteristics of pore structure

	Hg intrusion method				BET method	
	Pore volume [ml/g]	surface area [m <sup>2</sup> /g]	macropore diameter [μm]	mesopore diameter [nm]	surface area [m <sup>2</sup> /g]	DH pore diameter [nm]
α-Al <sub>2</sub> O <sub>3</sub>	0.204	0.84	1.01	-	1.79	-
Ni/Bimodal	0.175	3.31	0.92	7.5	5.84	4.0
γ-Al <sub>2</sub> O <sub>3</sub>	-	-	-	-	252	4.0

## List of figures

Fig.1 Schematic concept of a catalytic membrane (a) and a bimodal catalytic membrane (b). (Figure 1 (a) indicates a conventional catalytic membrane with a monomodal catalytic structure, while Figure 1 (b) shows a bimodal catalysts in which mesoporous materials are impregnated in the macroporous supports.)

Fig.2 Schematic diagram of the experimental apparatus used in the steam reforming of methane.

Figure3 SEM cross-sections of an  $\alpha$ -Al<sub>2</sub>O<sub>3</sub> support (a), and a Ni-impregnated  $\alpha$ -Al<sub>2</sub>O<sub>3</sub> support (b), and a bimodal catalytic support (c).

Fig.4 Pore size distribution of an  $\alpha$ -Al<sub>2</sub>O<sub>3</sub> support (a) and a bimodal catalytic support (b). (A bimodal support: impregnated amount of NiO = 20 mg/g- $\alpha$ -Al<sub>2</sub>O<sub>3</sub>.)

Fig. 5 Hydrogen adsorption, BET surface area, and amount of NiO impregnated as a function of the amount of impregnated  $\gamma$ -Al<sub>2</sub>O<sub>3</sub>.

Fig. 6 A cross-sectional photo of a bimodal catalytic membrane.

Fig. 7 Gaseous permeances as a function of reciprocal permeation temperature before and after hydrothermal treatment (hydrothermal treatment was carried out at 50 kPa of steam and 500 °C for three hours)

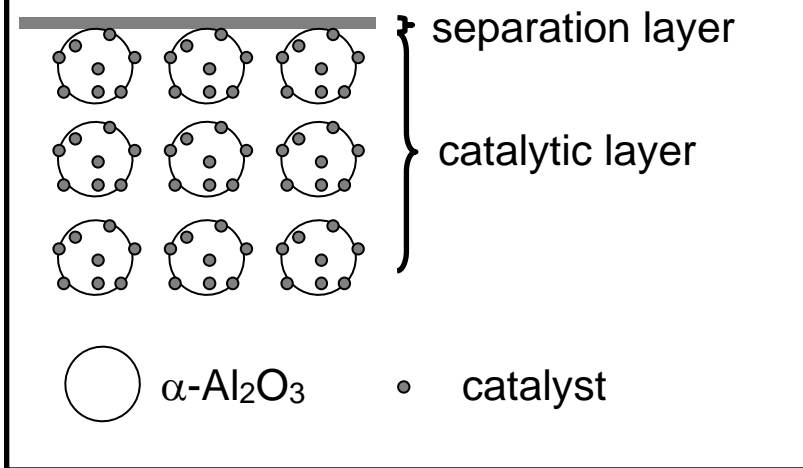
Fig. 8 Conversion of methane as a function of CH<sub>4</sub> feed flow rate for Ni/  $\alpha$ -Al<sub>2</sub>O<sub>3</sub> supports (NiO: 0.11, 0.21 g) (a) and Ni/ bimodal supports ( $\gamma$ -Al<sub>2</sub>O<sub>3</sub> 38, 9 mg; NiO 0.13, 0.127 g) (b). (Broken and dotted lines indicate equilibrium conversions at 100 and 120 kPa, respectively.)

Fig. 9 Time course for the permeance of the catalytic membrane (Permeate stream was evacuated after 160 min from 100 kPa to 20 kPa. CH<sub>4</sub> feed flow rate=6x10<sup>-6</sup> mol s<sup>-1</sup>; S/C=3; lines are calculated using H<sub>2</sub> permeance= 4.8x10<sup>-6</sup> m<sup>3</sup>m<sup>-2</sup>s<sup>-1</sup>kPa<sup>-1</sup>, separation factor of H<sub>2</sub> over N<sub>2</sub> ( $\alpha$  (H<sub>2</sub>/N<sub>2</sub>)) = 40, and  $\alpha$ (H<sub>2</sub>/H<sub>2</sub>O) =2.)

Fig. 10 Hydrogen yield and CH<sub>4</sub> conversion as a function of permeation number (Curves are calculated using p<sub>h</sub>=100 kPa, p<sub>l</sub>=20 kPa; S/C=3, H<sub>2</sub> permeance= 4.8x10<sup>-6</sup> m<sup>3</sup>m<sup>-2</sup>s<sup>-1</sup>kPa<sup>-1</sup>, separation factor of H<sub>2</sub> over N<sub>2</sub> ( $\alpha$  (H<sub>2</sub>/N<sub>2</sub>)) = 40, and  $\alpha$ (H<sub>2</sub>/H<sub>2</sub>O) = 2.)

Fig. 1

### Catalytic membrane



### Bimodal catalytic membrane

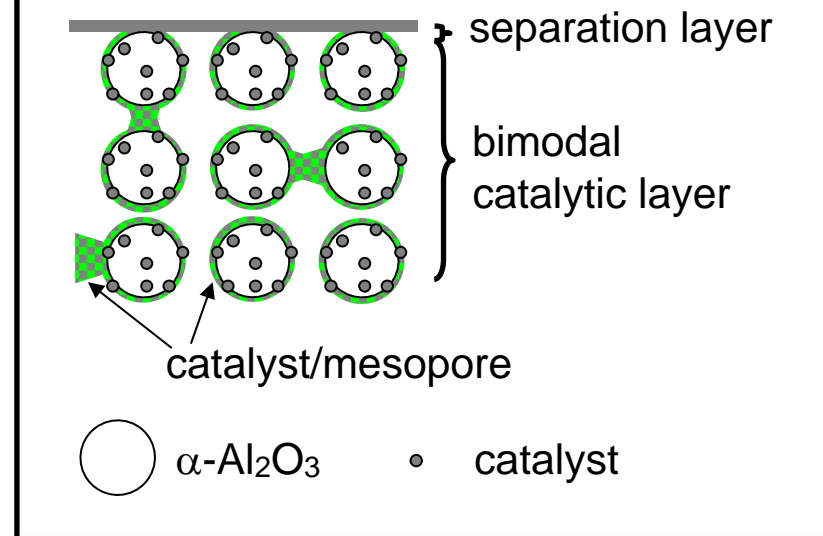




Fig. 2

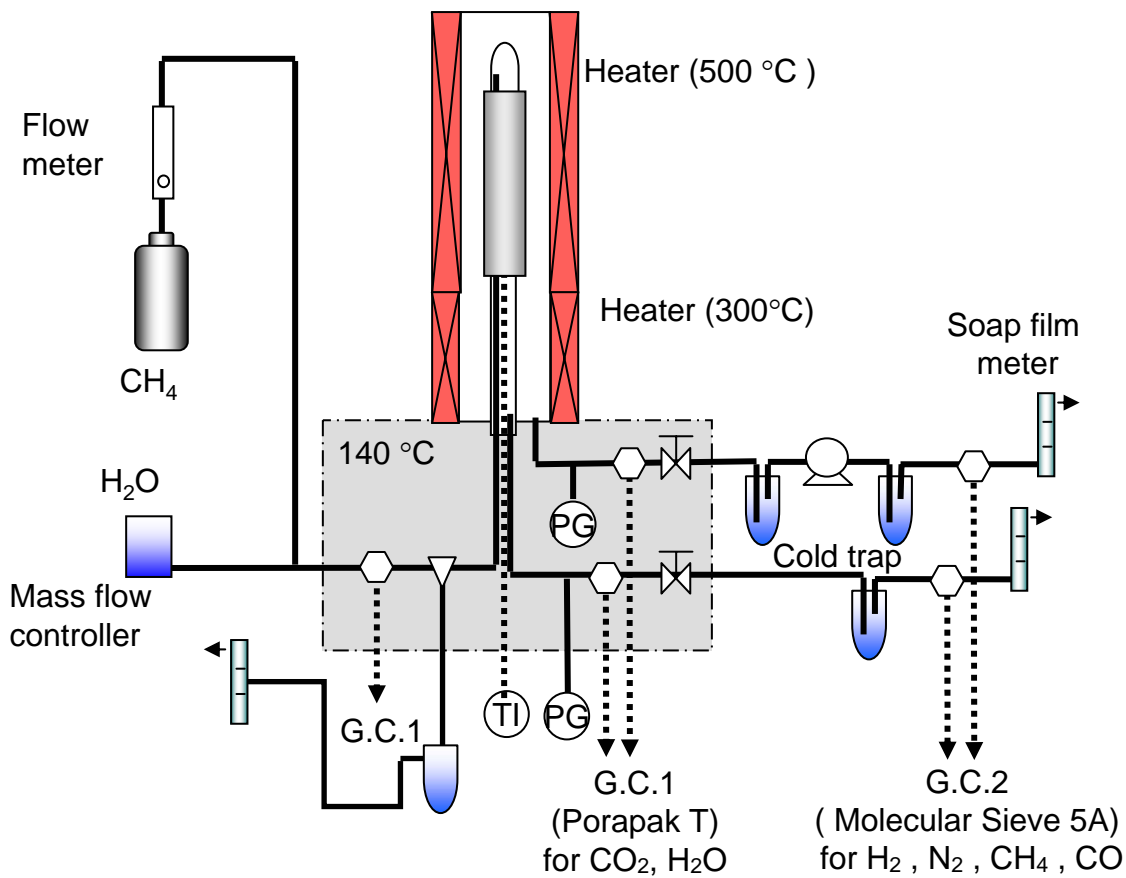
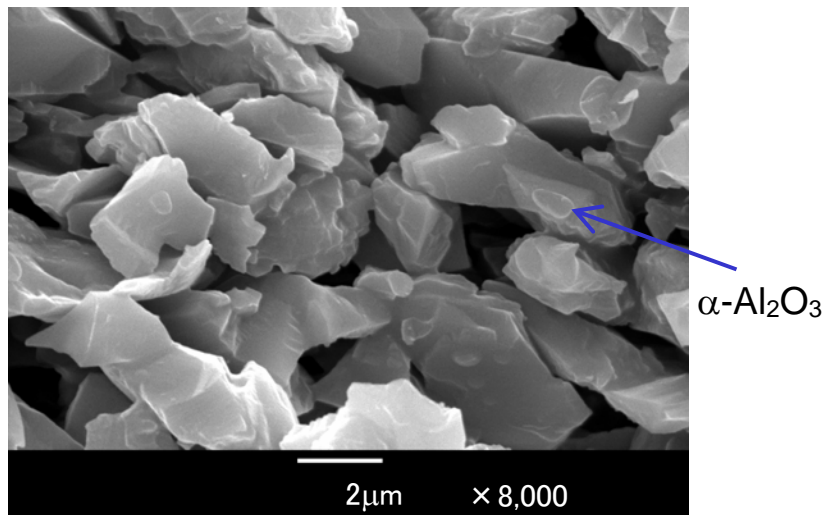
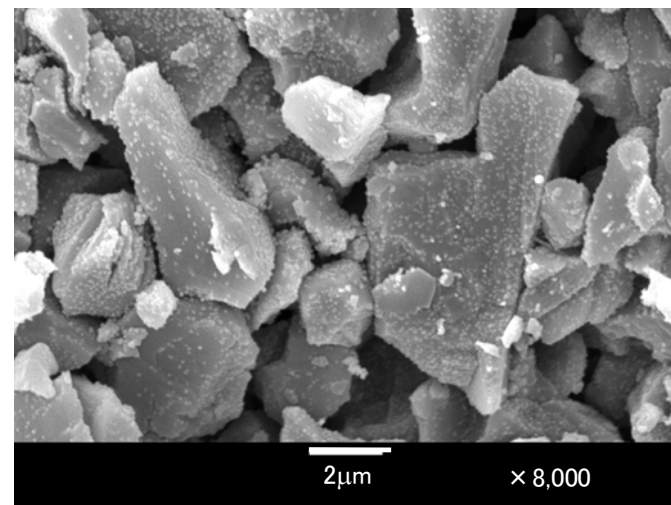


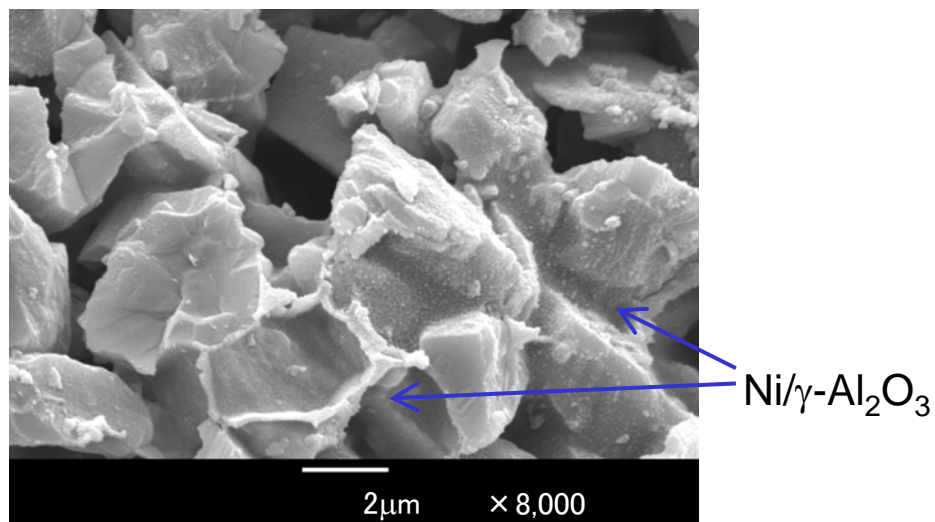
Fig. 3



(a)  $\alpha$ - $\text{Al}_2\text{O}_3$  support



(b) Ni/ $\alpha$ - $\text{Al}_2\text{O}_3$  support



(c) Ni/bimodal support (bimodal catalytic support)

Fig. 4

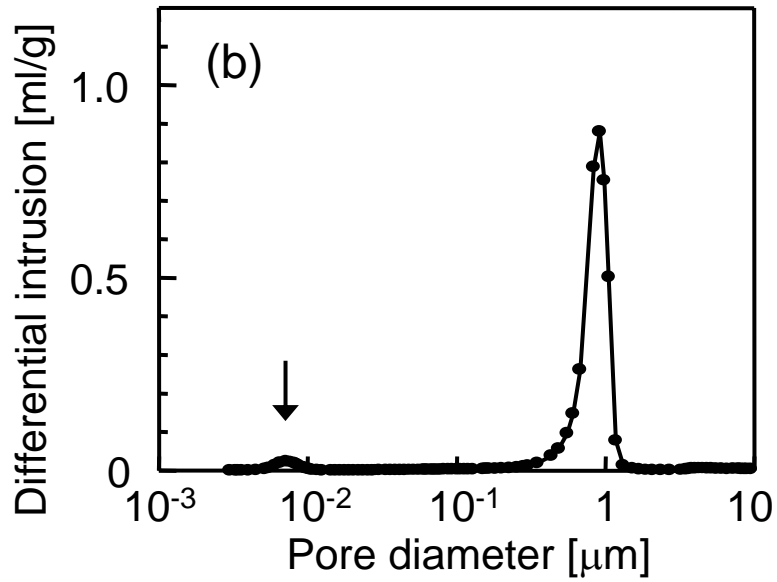
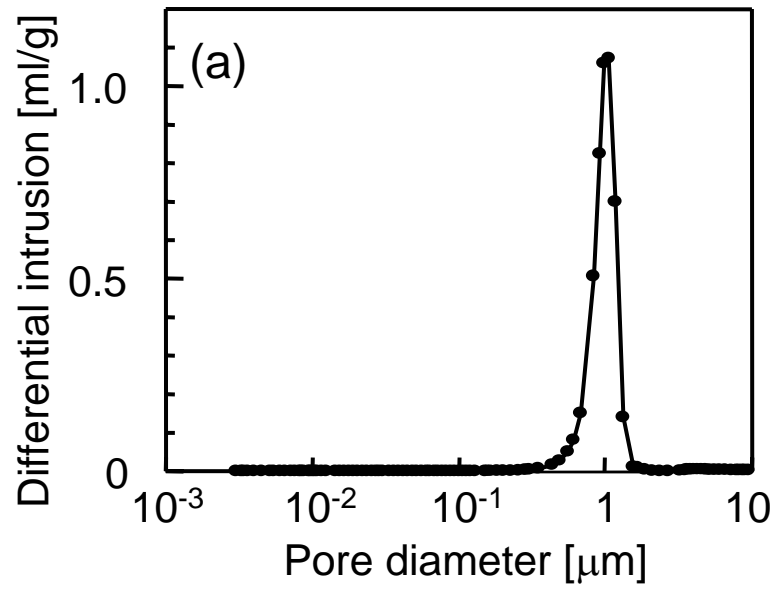


Fig. 5

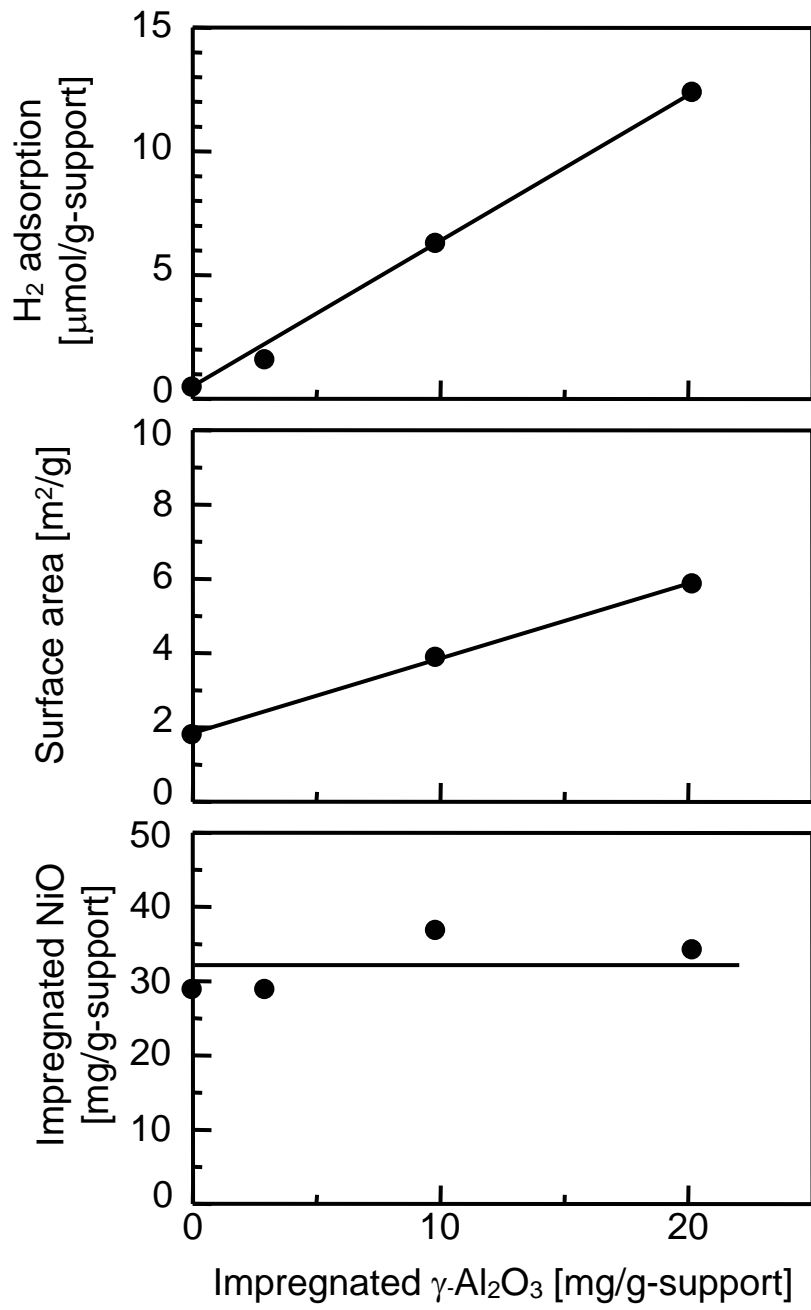
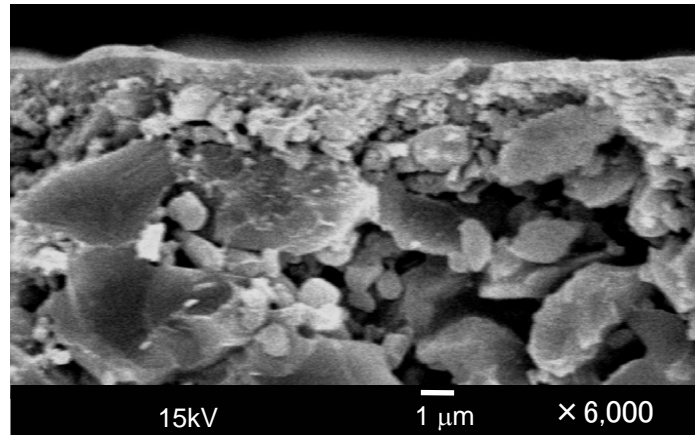


Fig. 6



} separation  
layer

} catalytic  
layer

Fig. 7

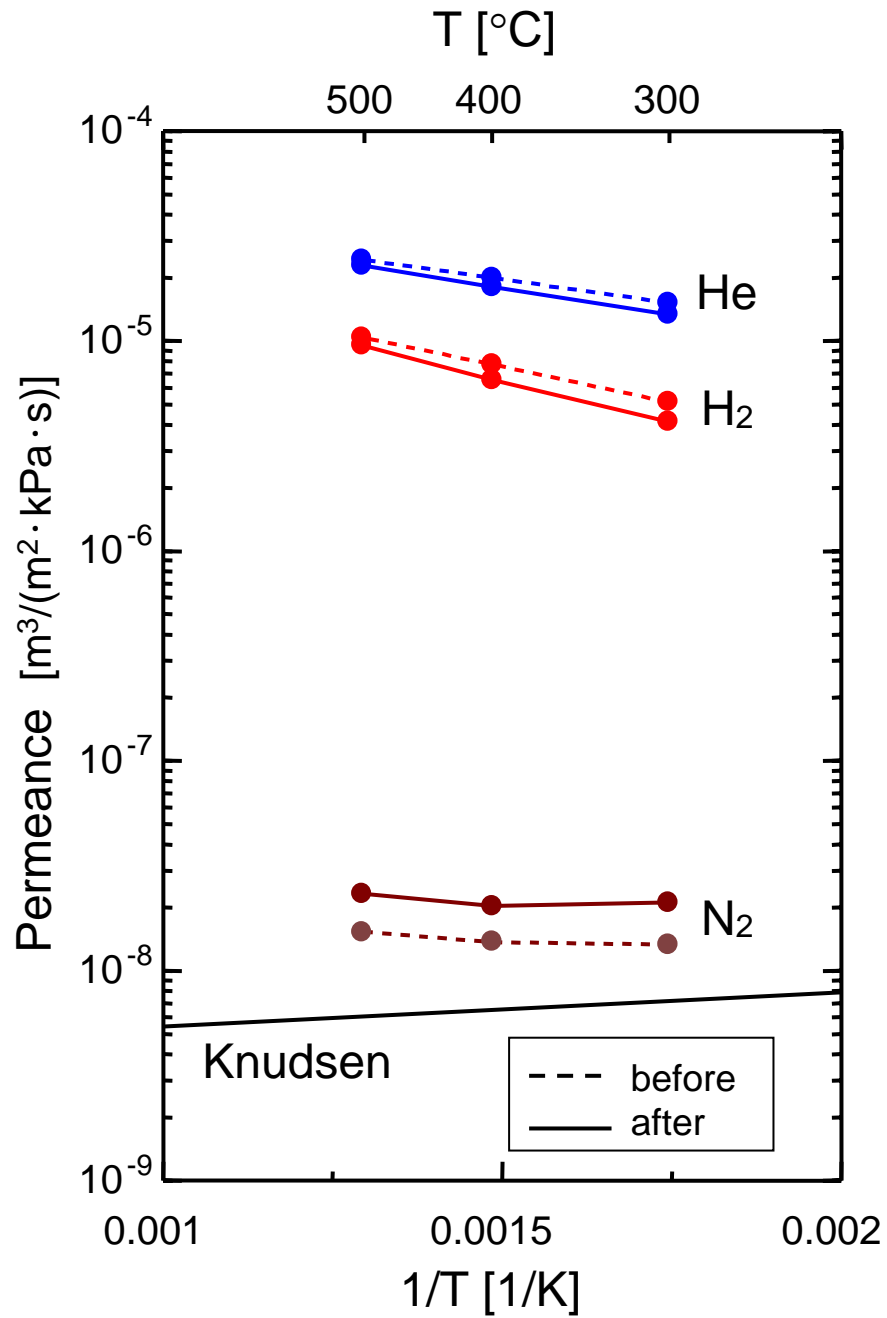


Fig. 8(a)

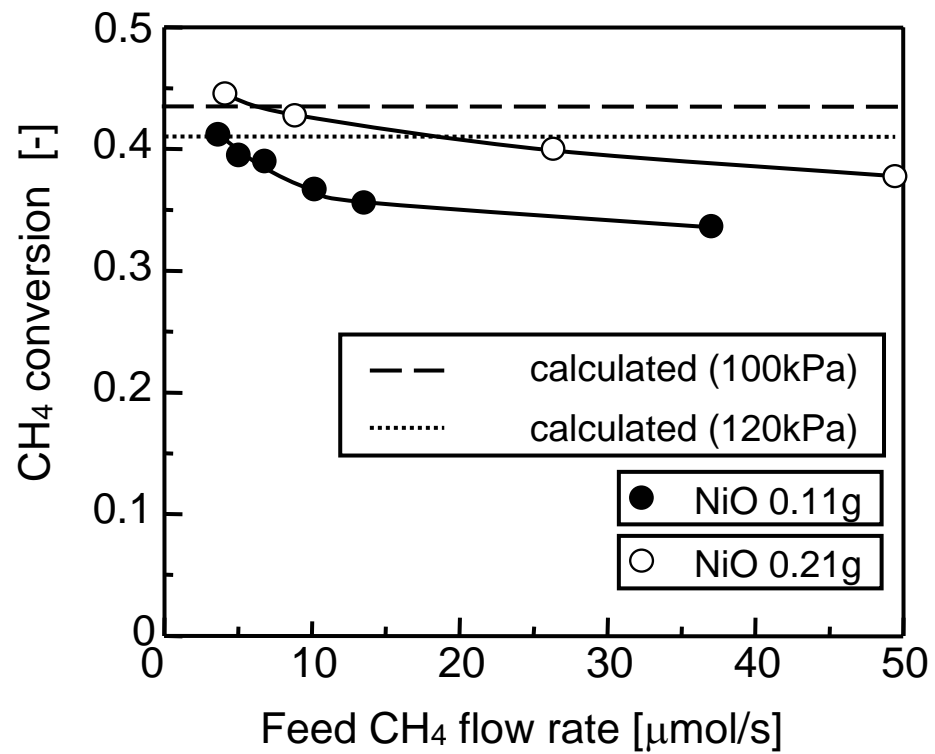


Fig. 8(b)

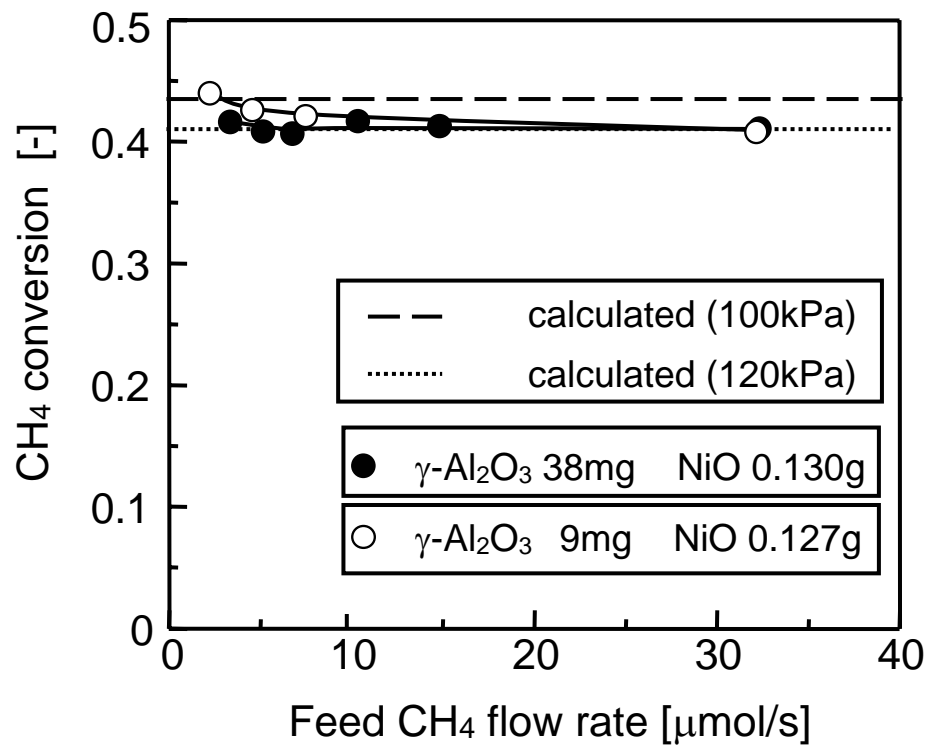




Fig. 9

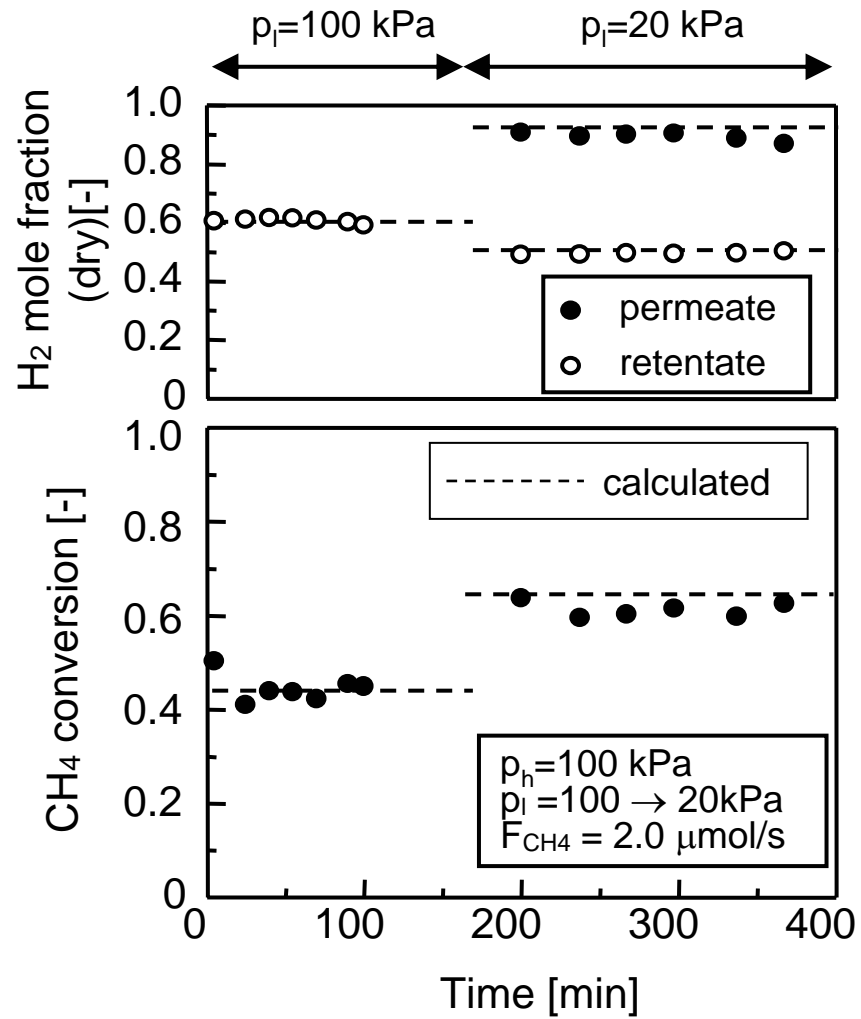


Fig. 10

